

Volume integration of fractal distribution networks

Walton R. Gutierrez*

Touro College, 27 West 23rd Street, New York, NY 10010

(Received 15 January 2002; revised manuscript received 22 May 2002; published 21 October 2002)

An approach based on integral calculus methods is developed in order to determine the volume of a distribution network with fractal characteristics. This approach introduces alternative useful techniques and concepts to the study of the self-similarity of fractal distribution networks. The application to the allometry of organs reveals other possible scaling for the bronchial tree and the kidney arterial tree of mammals.

DOI: 10.1103/PhysRevE.66.041906

PACS number(s): 87.19.Rr, 05.45.Df, 89.75.Hc

I. INTRODUCTION

The work of West *et al.* [1–3] made the connection between fractal networks and many allometric scaling laws of organisms. Turcotte *et al.* [4] proposed the theory of Tokunaga [4] to be a better model of fractal branching of distribution networks. A key aspect of these models is the evaluation of the network volume based on particular definitions of network branching that restrict possible applications to a few organ networks of mammals. Recently, various modifications to these previous models have been suggested by Dodds *et al.* [5] and Gutierrez [6].

A set of experimentally accepted and simple characteristics of distribution networks of organs [6,7] is part of the basis of this approach to the network volume. Starting from a proposed general formula and using a method of successive approximations, the volume of the network is calculated analytically in terms of various geometric functions representing some of the morphology of the network. The resulting network volume in the first order of approximation is used to develop a model of the scaling of the network volume that can be applied to organisms. A theoretical goal of the integration method is to describe distribution networks using mathematical concepts that overcome the restrictive and limiting self-similarity concepts so far used [1–4]. With this method, no particular branching patterns are needed to determine the volume of the network, branching patterns that in natural networks are usually much more complicated than simple fractals. A key analytic concept is the subdivision of the network volume into tiny filament volumes (Fig. 1). The description of the filaments requires the introduction of various functions and parameters that also describe a general type of fractal network. In this analysis, the circulation distance function (X_S) plays a significant role, a function that should prove quite useful in the measurements of many types of natural distribution networks. The integration method allows the introduction of optimization considerations, different from those so far implemented in existing models [1–5] such as, for example, the optimization of the circulation distance. A more complete account of the relation of the integration method to optimization conditions is beyond the goals of this article, but a useful example of a simple optimization consideration is carried out for the long range cir-

ulation distance in the discussion of the model's application to the lung and kidney (Sec. III). A notable outcome of this application is the fact that Euclidean exponents (1/3 or its multiples) can coexist with “remarkable” exponents (such as 1/4 or its multiples) for the same volume quantity. This result helps to remove a prevalent theoretical dichotomy between these two types of exponents that has been a persistent and troubling feature in most of the existing models of allometry [1,2,3,7]. As a more unifying fractal feature of the network, the concept of global self-similarity is introduced, which provides for a model that is in principle applicable to any organ network. Although more data than currently available are needed to further test the concepts here presented, the existing relevant allometric data of organs lend preliminary support to the proposed model (Tables I and II). Concurrently, the proposed model also yields other insights into what type of data correlations would be of immediate benefit to investigate (Sec. III).

II. INTEGRATION OF NETWORK VOLUME

An organ is represented by a volume V . A large portion of V ($\approx 80\%$ or more), named V_{TS} , is subdivided by a large

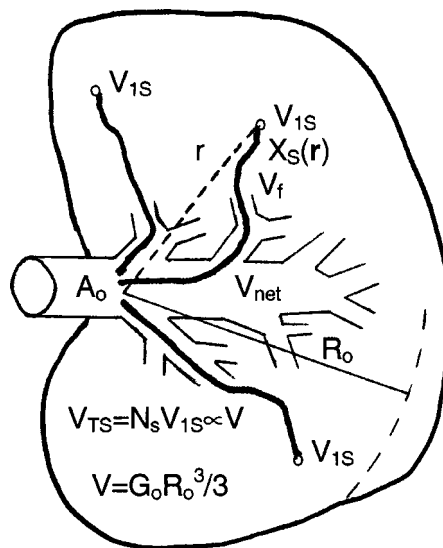


FIG. 1. Schematics of volume V showing the main variables. The illustrated black filament has a volume V_f and a length $X_S(\mathbf{r})$. The total volume of all filaments is V_{net} .

*Electronic address: waltong@touro.edu

TABLE I. Determination of b as $A_0 \propto V^b \propto M_B^{cb}$. A_0 , cross section area; V , organ volume; M_B , body mass; ND, no data.

A_0	cb^a	c^a	b
Mammals			
Trachea	0.78	1.06 (lung)	0.78/1.06=0.74
Renal artery	0.61	0.85 (kidney)	0.61/0.85=0.72
Birds			
Trachea	0.70	0.97 (lung)	0.70/0.97=0.72
Renal artery	ND ^b	0.91 (kidney)	ND
			average $b=0.73$

^aFrom [7], Tables 3-4, 5-3, and 5-6.

^bIf $b=0.73$ is constant, then this exponent can be predicted to be 0.66.

number N_s of very small and equal sites, each with a volume V_{1S} , that is, $V_{TS}/N_s = V_{1S}$. These sites are serviced by a distribution network of volume V_{net} . There may be several networks in a particular organ. For example, in the lung there are the arterial and the bronchial networks. To simplify, but without loss of generality, we shall assume there is one network in the organ volume,

$$V = V_{net} + V_{TS}. \tag{1}$$

For example, V can represent the kidney volume and N_s the number of nephrons in the kidney (human kidney, $N_s \approx 10^6$). The average volume of one nephron is V_{1S} and $V_{TS} = N_s V_{1S}$ is the volume of all nephrons. V_{net} may be the volume of the arterial network supplying the nephrons [6]. A useful concept is the density of the distribution of sites D_S which, being nearly uniform, can be defined as

$$D_S = N_s / V_{TS} = C_0 N_s / V, \tag{2}$$

where $V = C_0 V_{TS}$. Since V_{TS} is a large part of V , it is assumed to be proportional to V , which is supported by allometric data [7].

The main goal of this section is to describe and quantify the volume of a distribution network that looks like a high

TABLE II. Scaling of network volume (V_{net}). $V_{net} \propto M_B^{cw}$ $= M_B^{1.06c} = M_B^{c \cdot w}$; $w = b + 1/3$. ND, no data. See Table I for initial data.

Network description	Previous model [1]	Observed (expt)	Model proposed 1.06c
Mammals			
Bronchial	1.0	1.06–1.18 ^a	1.12
Kidney arterial	ND	ND	0.90
Birds			
Bronchial	ND	0.97–1.09 ^a	1.03
Kidney arterial	ND	ND	0.96

^aDue to the lack of experimental data on V_{net} , the observed scaling of bronchial tree volume is estimated to be between lung volume (low value) and trachea volume (high value) [7].

order fractal, that is centrally supplied or drained, and that services a complete volume through the sites. In the descriptions of fractal distribution networks given below, the following hypothesis is made: if all parameters and functions are specified, the resulting network describes a statistical average of a large ensemble of networks, rather than a single network, consistent with a set of design constraints. This interpretation is supported by numerical simulations of network designs [8,3] and by network error tolerance considerations [9]. Next, a general construction of the integration method is shown, followed by a method of successive approximations for the relevant functions. If each site volume V_{1S} is equally supplied, then a filament volume V_f is defined by linking an area A_0/N_s of the initial branch cross section, to the cross section area A_s connected to V_{1S} (Fig. 1). For example, A_0 can be the cross section area of the renal artery and A_s the cross section area of the arteriole feeding a nephron. The filament volume V_f is not an element of volume of the moving fluid, but an abstract way of subdividing V_{net} . The cross section area of V_f is in general a variable function represented by $A(X)$. The variable X is the partial length of the V_f volume, in the range of $0 \leq X \leq X_S(\mathbf{r})$, where X_S is the total length of V_f , which in turn depends on the spatial location of V_{1S} specified by the position vector $\mathbf{r} = (r_x, r_y, r_z)$. The function $X_S(\mathbf{r})$ is known as the circulation distance. The volume V_f of this abstract filament is

$$V_f(\mathbf{r}) = \int_0^{X_S(\mathbf{r})} A(X) dX, \quad A(0) = A_0/N_s, \quad A(X_S) = A_s. \tag{3}$$

Therefore the volume of the distribution network V_{net} is

$$V_{net} = \sum_I^{N_s} V_f(\mathbf{r}_i) = \int_V V_f(\mathbf{r}) D_S(\mathbf{r}) dV. \tag{4}$$

A key step is the substitution of the summation of all the filament volumes $V_f(\mathbf{r})$ by an integral using the general density $D_S(\mathbf{r})$ of the sites which, in the case of a constant density, is given by Eq. (2). In the case of a general density we would have $\int_V D_S(\mathbf{r}) dV = N_s$. Clearly a uniform constant density D_S throughout V is only an approximation, since there are no sites in the space occupied by V_{net} . This approximation would introduce a small error, since the network volume is a small part of the total volume. This error may be corrected somewhat by adjusting the integration by a constant factor C_1 that would be near 1. If D_S is a constant density, using Eq. (2) in Eq. (4)

$$V_{net} = C_1 C_0 (N_s / V) \int_V V_f(\mathbf{r}) dV. \tag{5}$$

The filament functions $A(X)$ and $V_f(\mathbf{r})$ play the role of test functions, modeling the geometry of the network in greater detail for a more specific organ or system. In general, we may assume that $A(X)$ is a monotonic function interpolating between $A(0)$ and $A(X_S) = A_s$; therefore, using the mean value theorem, the integral of $A(X)$ in Eq. (3) can be represented as

$$\begin{aligned} V_f(\mathbf{r}) &= [A(0)p_1 + A_s(1-p_1)]X_S(\mathbf{r}) \\ &= A(0)F_A(p_1)X_S(\mathbf{r}), \end{aligned} \quad (6)$$

where $0 \leq p_1 \leq 1$, and $F_A(p_1)$ is defined by Eq. (6).

For the volume V and the circulation distance X_S , spherical coordinates $\mathbf{r} = (r, \theta, \phi) = (r, \Omega)$ are chosen. An efficient network would have a circulation distance $X_S(\mathbf{r})$ as small as possible. The smallest possible value is the length $r = (r_x^2 + r_y^2 + r_z^2)^{1/2}$, which $X_S(\mathbf{r})$ cannot equal. Therefore a simple method of successive approximations can be made with the powers of r ,

$$X_S(\mathbf{r}) = f_1 r^{u-} + f_2 r^v x_2(\theta, \phi) > r, \quad (7)$$

where the first term is the main contribution, and f_2 is a small parameter. The surface of V is modeled by the function $R(\Omega) = R(\theta, \phi) = R_0 H(\theta, \phi)$, where $0 < R_0$, $0 < H(\theta, \phi) \approx 1$, and from Eqs. (5)–(7)

$$V_{\text{net}} = C_0 C_1 F_A(A_0/V) \int_{\Omega} \int_0^{R(\Omega)} X_S(\mathbf{r}) r^2 dr d\Omega, \quad (8)$$

where the volume $V = \int \int (\int_0^{R(\Omega)} r^2 dr) \sin \phi d\theta d\phi = (R_0^3/3) \int_{\Omega} H^3(\Omega) d\Omega = (R_0^3/3) G_0$, and G_0 is the angular integration. Similarly, using Eq. (7) in the integral over $X_S(\mathbf{r})$, $\int_{\Omega} \int_0^R X_S(\mathbf{r}) r^2 dr d\Omega = f_1 (R_0^{3+u}/(3+u)) \int_{\Omega} H^{3+u}(\Omega) d\Omega + f_2 (R_0^{3+v}/(3+v)) \int_{\Omega} x_2(\Omega) H^{3+v}(\Omega) d\Omega$. Using these last results in Eq. (8),

$$\begin{aligned} V_{\text{net}} &= C_0 C_1 F_A A_0 [3 G_1(u) f_1 R_0^u / (3+u) \\ &\quad + 3 G_2(v) f_2 R_0^v / (3+v)], \end{aligned} \quad (9)$$

where $G_1(u) = \int_{\Omega} H^{3+u}(\Omega) d\Omega / G_0$ and $G_2(v) = \int_{\Omega} x_2(\Omega) H^{3+v}(\Omega) d\Omega / G_0$ are the form factors remaining from the angular integrations. This result for V_{net} also has a first main term and a second term proportional to the small parameter f_2 . The G_k factors contain the contribution of the organ form to the network volume. Taking now the approximation of only the first term ($f_2 = 0$), we see that the network volume is proportional to the long range circulation distance $X_S(R_0) = f_1 R_0^u$ shown in Eq. (7), that is,

$$V_{\text{net1}} = 3 C_0 C_1 F_A G_1(u) A_0 X_S(R_0) / (3+u) = C_2 A_0 X_S(R_0), \quad (10)$$

where C_2 is defined by Eq. (10). This last equation is the main result for the first order approximation of the network volume.

III. APPLICATION TO ORGANS

Before the main allometric application is considered, it is important to note here that the network volume receives contributions from the organ external form or boundary through the G_k form factors [Eq. (9)]. As far as this author knows, the network's external boundary has not been part of previous fractal theoretical analyses. A numerical simulation [10] of distribution networks did show the qualitative effect on the

network of the overall exterior form of the network (the organ form). Clearly, this topic can be investigated farther with the help of numerical simulation methods.

A thorough correlation of the mathematical model of the previous section with the experimental data is not yet possible due to the lack of experimental information on the circulation distance function [Eq. (7)]. I have seen only one experimental reference that measures the circulation distance in arborescent sponges [11], where it is found apparently that the circulation distance follows mainly a power function as given in Eq. (7). However, additional comparison in this case is not possible because arborescent sponges are low order fractals where the space filling sites premise is not applicable. Although the data sets of the distribution networks of organs of animals are very incomplete, this is still a very desirable topic that we can discuss meaningfully. The main point here is to show how future experimental data may select or improve the existing models.

Previous models of network volume [1–4] were based on the condition of constant ratio self-similarity, where all the ratios N_{k+1}/N_k , A_{k+1}/A_k , and L_{k+1}/L_k are constant. These are the ratios of the number of branches, cross section area of branches, and lengths of branches, respectively, which are constant in relation to the generation number $k = 0, 1, 2, \dots, s$. Under this condition, the network volume (V_{netp}) is given by $V_{\text{netp}} = C_{\text{cr}} A_0 L_0$, where L_0 is the length of the first and largest branch of the network and C_{cr} depends on other parameters. Also, under constant ratio self-similarity, the maximum circulation distance $X_{\text{max}} = \sum_0^s L_k$ is proportional to L_0 and therefore X_{max} and L_0 will scale in the same way in relation to organ volume. This last particular condition imposed by constant ratio self-similarity is unlikely to be valid in the lung as we shall argue below. In the integration method the relation between X_{max} and L_0 is mostly irrelevant in the determination of the volume. Clearly, X_{max} is directly related to $X_S(R_0)$. Therefore Eqs. (9) and (10) represent a generalization applicable to a class of networks that may not be constant ratio self-similar, since no assumptions on branching patterns have been made here.

We can use mammal allometric data for the trachea and lung to show some of the potential problems of $V_{\text{netp}} = C_{\text{cr}} A_0 L_0$. The data are from Calder's tables [7], and are also part of Tables I and II. Taking the trachea as the first stage of the lung [1] the cross section is $A_0 \propto M_B^{0.78}$, and the length is $L_0 \propto M_B^{0.40}$ (M_B = body mass); therefore the bronchial network $V_{\text{netp}} \propto M_B^{1.18}$ which now has to be compared to the scaling of the lung volume, $V \propto M_B^{1.06}$. $M_B^{1.18}$ and $M_B^{1.06}$ are an unlikely combination of scaling in the same lungs. Only actual allometric data on the bronchial tree could resolve this question.

From another perspective the trachea provides supporting evidence for the Euclidean optimization argument applied below. Here, the Euclidean scaling of a length L of a part of an organ in relation to the same organ volume V is defined as $L \propto V^{1/3}$. In this sense the trachea of mammals is altogether Euclidean. Since the trachea volume is $V \propto M_B^{1.18}$, then its length $L \propto V^{0.40/1.18} = V^{0.34}$, and its diameter $D \propto A_0^{1/2} \propto V^{0.39/1.18} = V^{0.33}$. The same observation can be made of the

trachea of birds ($L \propto V^{0.36}, D \propto V^{0.32}$). These data show that there are well defined Euclidean exponents in some circulatory organs. Although the trachea has been used as the first stage of the bronchial tree [1], from the point of view of the integration method a better choice would be the first bronchus, but there are no allometric data on the first few stages of the bronchial tree. Therefore, we continue to use the trachea as a surrogate for the first bronchus.

As shown by Dodds *et al.* [5] the theoretical link between optimal networks and constant ratio self-similarity remains tentative and a rather difficult mathematical problem. Experimentally, constant ratio self-similarity may be a good approximation in the arterial tree of the lung [4]; however, significant departure from constant ratio self-similarity has been observed in the bronchial tree [9] and in arterial trees of the heart [12]. To go beyond the restrictions imposed by constant ratio self-similarity the following model is introduced. Based on Eq. (10), it is proposed that under large variations of organ volume V , such as from a mouse to a horse, $V_{\text{net}} = C_2 A_0 X_S(R_0)$ where $X_S(R_0) \propto R_0^u \propto V^{u/3}$, $A_0 \propto V^b$, and $C_2 \propto V^z$; thus $V_{\text{net}} \propto V^w$, and $w = b + z + u/3$. Networks conforming to these last conditions are designated here as globally self-similar. To apply global self-similarity to the kidney and lung, it is assumed as an approximation that C_2 is invariant ($z = 0$). In the supplying networks of the kidney and lung of mammals a good approximation is $b = 0.73$, and the remarkable constancy of $b = 0.73$ for centrally supplied organs is shown in the relevant data displayed in Table I. The exponent b has other important implications for the various scaling laws of organs, a topic that is more fully discussed in [6].

To determine u , the following optimality argument is applied. The length of $X_S(R_0)$ is the length of a continuous curve formed by the finite union of a set of smooth curve segments. This curve goes from the center of the organ to a point on its surface. The minimization of the length of this curve is found in the fact that this curve does not loop or backstep and sidesteps only at a small angle. These descriptions identify a large set of curves. The length of a typical curve in this set can be safely estimated to be proportional to $V^{1/3}$, or very nearly so, as shown by a more detailed argument given in the Appendix. Therefore, from Eq. (7) we have $X_S(R_0) = f_1 R_0 \propto V^{1/3}$ ($f_1 > 1$), setting $u = 1$. We find $V_{\text{net}} \propto V^w = V^{1.06}$. To link the latter with allometric data, we use the experimental scaling of organ volume to body mass (M_B): $V \propto M_B^c$ (for example, $c = 0.85$ for the kidney of mammals). In this way, $V_{\text{net}} \propto M_B^{wc} = M_B^{1.06c}$. These results are summarized in Table II. We may try to extend these results to other blood distribution networks, but allometric data are very minimal in this respect. Some organ networks of mammals and birds may have reached a degree of geometrical optimization described by the Euclidean scaling ($V^{1/3}$) of $X_S(R_0)$. Measurements of X_S for organs are not yet available. The previous estimate [1] was $X_S \propto M_B^{0.25}$, which in this model is $X_S \propto M_B^{uc/3} = M_B^{c/3}$.

So far, this discussion and the data presented clearly show that many of the exponents are not “universal” multiples of $1/4$ as previously suggested [1–3]. Rather, there is a more

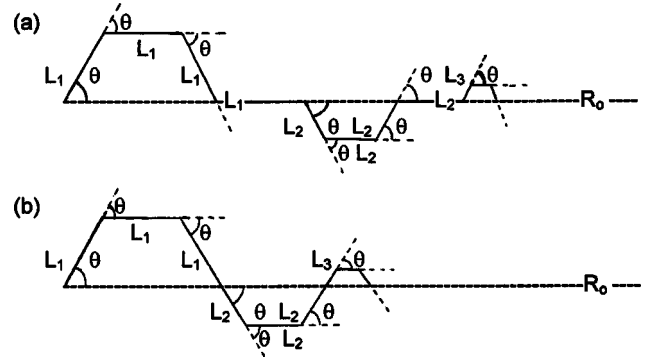


FIG. 2. Models of a line followed by a filament volume. The sum of all L_k is $X_S(R_0)$.

diverse mixture of exponents applicable to specific categories of animals and organs. Presumably the value $b = 0.73$ would be modeled as a by-product of Kleiber’s law models [1–4]; however, this item remains controversial [5]. Theoretically speaking, the multiple values of c represent a much larger problem. The values of c convey the relative size, and need of a whole body, for each specific organ in groups of similar organisms.

Since we have found that $V_{\text{net}} \propto V^w = V^{1.06}$, this poses the following question. If $V = V_{\text{net}} + V_{TS}$ and $V_{TS} \propto V$ [Eqs. (1) and (2)], how is it that $V_{\text{net}} \propto V^w$, with $w > 1$? The answer is based on the very good approximation for small x and p given by $V \approx [pV^{1+x} + (1-p)V^{1-x}]/V^{(xy/2)\ln V}$, where $y = p/(1-p)$, and $V_{\text{net}} = pV^{1+x}$. This formula can be derived using the conventional expansion $V^H = e^{H \ln V} = 1 + H \ln V + (H \ln V)^2/2 + \dots$. For example, if $x = 0.06$, $p = 1/7$, then $y = 1/6$, and $V \approx (0.143V^{1.06} + 0.857V^{0.99})/V^{0.0003 \ln V}$. There is a small error even if the term $1/V^{0.0003 \ln V}$ is approximated by 1. By doing so, in the range of V of $10^{\pm 5}$, there is a maximum percent error of V of 4%. In allometric data these small deviations, such as $V^{0.995 \pm 0.005}$ or $V(1 \pm 0.04)$, are essentially undetectable.

APPENDIX

Here we make some estimates on the range of variation of X_S in relation to R_0 and V . The type of curve of which $X_S(R_0)$ is the length can be approximated as a sequence of straight segments with sidesteps at an average angle θ . The length would depend on this angle and on the degree of corrugation of the set of segments. Two simple models are shown in Fig. 2. From the model of Fig. 2(a) we obtain $X_S(R_0) = 4 \sum L_k$, $R_0 = 2(1 + \cos \theta) \sum L_k$, and therefore

$$f_{1a} = X_S(R_0)/R_0 = 2/(1 + \cos \theta). \quad (\text{A1})$$

From the model of Fig. 2(b) we obtain $X_S(R_0) = 3 \sum L_k$, $R_0 = (1 + 2 \cos \theta) \sum L_k$, and therefore

$$f_{1b} = X_S(R_0)/R_0 = 3/(1 + 2 \cos \theta). \quad (\text{A2})$$

Now we make an estimate of the most likely range for the angle θ . Angles very near 0° or 90° are entirely unrealistic. If we choose the generous range of $30\text{--}70^\circ$ we get a percent

variation for f_{1a} of 39% and for f_{1b} of 62%. Let us assume a maximum percent variation of f_1 of 60% and calculate the impact on the exponent u of the scaling law (Sec. III), $(V/V')^{u/3} = X_S(R_0)/X'_S(R_0) = f_1 R_0 / f'_1 R'_0 = (f_1/f'_1)(V/V')^{1/3}$. The variation of f_1 is represented by $f_1/f'_1 = (1.6)^{\pm 1}$. A typi-

cal variation of V , for example, in mammals is of the order of $V/V' = 10^6$, that is, from shrew (≈ 5 g) to elephant ($\approx 5 \times 10^6$ g). Therefore we obtain $10^{6u/3} = (1.6)^{\pm 1} 10^{6/3}$, or $u = 1 \pm 0.5 \log(1.6) = 1 \pm 0.1$, that is, the parameter u has an estimated maximum change of 10% around 1.

-
- [1] G. B. West, J. H. Brown, and B. J. Enquist, *Science* **276**, 122 (1997).
- [2] G. B. West, J. H. Brown, and B. J. Enquist, *Nature (London)* **400**, 664 (1999).
- [3] *Scaling in Biology*, edited by J. H. Brown and G. B. West (Oxford University Press, New York, 2000).
- [4] D. L. Turcotte, J. D. Pelletier, and W. I. Newman, *J. Theor. Biol.* **193**, 577 (1998); E. Tokunaga, in *Research of Pattern Formation*, edited by R. Takaki (KTK Scientific Publishers, Tokyo, 1994), pp. 445–468.
- [5] P. S. Dodds, D. H. Rothman, and J. S. Weitz, *J. Theor. Biol.* **209**, 9 (2001).
- [6] W. R. Gutierrez (unpublished).
- [7] W. A. Calder, *Size, Function, and Life History* (Dover, New York, 1996).
- [8] W. Schreiner, F. Neumann, M. Neumann, A. End, and S. M. Rodler, *J. Theor. Biol.* **187**, 147 (1997).
- [9] M. F. Shlesinger and B. J. West, *Phys. Rev. Lett.* **67**, 2106 (1991).
- [10] W. Schreiner *et al.*, in *Scaling in Biology* (Ref. [3]).
- [11] E. R. Abraham, *Mar. Biol. (Berlin)* **138**, 503 (2001).
- [12] M. Zamir, *J. Theor. Biol.* **197**, 517 (1999).